International Journal of Physics and Mathematics
www.physicsjournal.net
Online ISSN: 2664-8644, Print ISSN: 2664-8636
Received: 20-04-2022, Accepted: 21-05-2022, Published: 23-05-2022
Volume 4, Issue 1, 2022, Page No. 40-46

Facile synthesis, tetragonal crystal structure and tunable luminescence characteristics of synthesized phosphor for near-ultraviolet converted light emitting diodes and solid-state lighting devices

[1]Shashank Sharma, and [2]Sanjay Kumar Dubey

[1]Assistant Professor, Department of Physics, Govt. E. R. R. P.G. Science College, Bilaspur, Chhattisgarh, India

[2]Assistant Professor, Department of Physics, Dr. Radha Bai, Govt. Navin Girls College, Raipur Chhattisgarh, India

Abstract

The effect of concentration of Eu^{2+}-doped and Dy^{3+}-codoped on the photoluminescence properties of $Ca_2MgSi_2O_7$ is discussed. Through the implementation of a high-temperature solid-state reaction process, the powder samples were formed. The structural, optical characterisation, and chemical composition of produced powder samples have been determined using X-ray diffraction (XRD), Fourier transform infrared (FT-IR), and CIE colour coordinates analysis. Phase Identification was done by X-ray diffraction analysis and its results revealed tetragonal, akermanite structure with a space group $P\bar{4}21$ m. This structure is a member of melilite group. Nowadays, a significant amount of attention has been placed on researching the chemicals belonging to the melilite group. The estimated crystallite size (D) is ~42 nm. Photoluminescence (PL) emission and photoluminescence excitation (PLE) spectra were used to analyse optical characteristics. At wavelengths of 525 nm, the synthesized phosphor exhibits a greater PL emission intensity under UV excitation at 396 nm, which suits the visual perception of the human eye very well. The $Ca_2MgSi_2O_7$:Eu^{2+}, Dy^{3+} phosphor exhibits improvement in PL intensity and quenching occurs at 2 mol % doping concentration of Dy^{3+} ions and 0.5 mol % fixed doping concentration of Eu^{2+} ions. The synthesized phosphors may be potentially beneficial for solid-state lighting devices, depending on the specific the PL results. The synthesised phosphor's XRD, FTIR, PL, and CIE Chromaticity coordinates are also presented in this research investigation.

Keywords: $Ca_2MgSi_2O_7$, Eu^{2+}, Dy^{3+} phosphor, photoluminescence, solid-state reaction technique, X-ray diffraction (XRD), Fourier Transform Infrared (FT-IR) Spectroscopy, CIE colour coordinates

1. Introduction

To analyze the chemical structure and actual composition of the synthesized materials, researchers can use the Fourier transform infrared (FTIR) technology, an effective spectroscopic and significant analytical approach. For researchers, it's one of the most crucial analytical methods. With the aid of an infrared laser beam, this sort of analysis can be used to characterise and pinpoint the functional groups present in a variety of material samples, including solids, liquids, solutions, pastes, powders, films, fibres, and gases [1]. Each bond in a molecule is tested for IR absorption by an infrared spectroscopy, which yields a spectrum that is often expressed as a percentage of transmittance vs wavenumber (cm^{-1}). A broad spectrum of compounds with covalent bonds have been demonstrated to absorb electromagnetic radiation in the IR band [2]. The atomic vibrations of a molecule in the sample are then affected by the IR radiations, leading to a specific energy absorption and/or transmission. As a result, the FTIR may be employed to identify certain chemical vibrations that the sample contains [3]. The actual structural and chemical compositions of the elements exist in a powder material sample can be determined in the finger print infrared region (4000 to 400 cm^{-1}) and the functional group region (1400 to 400 cm^{-1}). In this present investigation, the FTIR spectra of $Ca_2MgSi_2O_7$:Eu^{2+}, Dy^{3+} powder sample have been studied. Under which the presence of chemical elements like Ca^{2+}, Mg^{2+}, Si^{4+}, Eu^{2+} and functional groups like Hydroxyl (O-H) and carbonate (CO_3^{2-}) as well as different chemical bonds such as Mg-O, Ca-O, Si-O_b-Si were successfully detected. Due to various their excellent optical characteristics, high physical-chemical stability, resistance to water, and robust crystal structures, silicates make great candidates to be employed in stable host structures [4, 5].

Considering that perhaps the ionic radii of Eu^{2+}, Ca^{2+}, and Dy^{3+} ions are 1.25 Å, 1.12 Å, and 0.97 Å, respectively, and exactly match, Eu^{2+} and Dy^{3+} ions are expected to occupy Ca^{2+} sites in the $Ca_2MgSi_2O_7$:Eu^{2+}, Dy^{3+} host [6]. Eu^{2+} and Dy^{3+} ions do not incorporate Mg^{2+} because the ionic radius of Mg^{2+} (0.72 Å) is far smaller than that of Eu^{2+} ions [7].

The prepared $Ca_2MgSi_2O_7$:Eu^{2+}, Dy^{3+} phosphor was excited at 396 nm and their corresponding emission spectra were recorded at bright green (525 nm) spectral line peaking due to the $^4F_{9/2} \rightarrow {}^6H_{13/2}$ transitions. Bright green, because it has the wavelength that human eyes seem to be most sensitive, serves to ensure effective and efficient emission colour. Luminous watches and devices have been constructed to use these pigments. So far, there is currently an important requirement for the development of a long phosphorescent phosphor that seems to be

radioactive-free owing to safety and environmental concerns. The results from this research demonstrate that this phosphor is a viable choice for implementation in light emitting diodes and solid-state lighting display devices.
Using nominal compositions of $CaCO_3$, $MgCO_3$, and SiO_2 as raw materials for the host and Eu_2O_3 and Dy_2O_3 as activator ions as well as H_3BO_3 as flux which were employed in this experiment, we report the structural and luminous features of Eu^{2+}-doped and Dy^{3+}-codoped silicate powder in the present investigation. In the host crystal lattice site, the activator ion is doped with 0.5 mol% Eu^{2+} ions and codoped with 2 mol% Dy^{3+} ions to investigate the impact of doping concentration.

2. Experimental Details

2.1 Phosphor Synthesis Process

Stoichiometric mixtures with nominal composition of $CaCO_3$ (Calcium Carbonate), $MgCO_3$ (Magnesium Carbonate), SiO_2 (Silica Oxide), as highly pure raw materials for the host and Eu_2O_3 (Europium Oxide) and Dy_2O_3 (Dysprosium Oxide) as activator ions as well as H_3BO_3 (Boric Acid) added as a flux were well synthesized with the help of conventional solid-state reaction technique. Eu^{2+} ions at a doping concentration of 0.5 mol% and Dy^{3+} ions at a concentration of 2 mol% were added to the host samples. All of the aforementioned chemical reagents were analytical-grade and with 99.99% purity. An agate mortar and pestle were used to thoroughly grind these raw ingredients into the desired ratio. The mixture is pre-fired at 950^0C and then completely burned for 3 hours at 1170^0C in a weak reducing environment with burning charcoal.
The entire process's chemical response can be summarized as follows:

$$CaCO_3 + MgCO_3 + SiO_2 + H_3BO_3 \rightarrow Ca_2MgSi_2O_7 + CO_2 (\uparrow) + O_2 (\uparrow) \quad (1)$$

$$CaCO_3 + MgCO_3 + SiO_2 + Eu_2O_3 + Dy_2O_3 + H_3BO_3 \rightarrow Ca_2MgSi_2O_7{:}Eu^{2+}, Dy^{3+} + CO_2 (\uparrow) + O_2 (\uparrow) \quad (2)$$

2.2 Phosphor Characterization Techniques

In the order to explore the relationship, a comprehensive evaluation of the structural, morphological, and optical characteristics of the formed powder sample with stoichiometric ratios of synthetic phosphors is described. 4mg of the phosphor was used for each measurement. Powder X-ray diffraction (XRD) was implemented to evaluate the phase composition, purity, and crystal structure of the as-prepared phosphors in order to analyse their structural characteristics. The XRD pattern has been obtained from Bruker D8 Advanced X-ray powder diffractometer using Cu-K_α radiation and the data were collected over the 2θ range 10^o-80^o. FTIR spectra were recorded with the help of Bruker FTIR Spectroscopy for investigating the finger print region (1400–400 cm^{-1}) as well as the functional groups (4000–1400 cm^{-1}) of prepared phosphor in middle infrared region (4000–400 cm^{-1}) by mixing the sample with potassium bromide (KBr). In order to evaluate the vibrational characteristics of the formed powder sample, FTIR spectra were also recorded. Using a Shimadzu RF-5301 PC Spectrofluorophotometer, the photoluminescence emission and excitation spectra were measured at room temperature. As an excitation source, a Xenon lamp was used. The colour coordinates for the spectrum energy distribution that are utilized by the Commission Internationale de l'Eclairage (CIE) (1931 chart).

3. Results and Discussion

3.1 Crystal Structure Analysis by XRD

Fig. 1 shows the crystal phase structure of the $Ca_{(2-x-y)}MgSi_2O_7$: xEu^{2+}, yDy^{3+} (x = 0.5 mol% and y = 2 mol%) powder sample determined from the X-ray powder diffraction pattern with Cu-K_α (λ = 1.5405 Å, at 40 kV, 40 mA). Comparison of the recorded powder XRD patterns with the standard JCPDS pdf file number #77-1149 shown good agreement and well matched. The XRD data were measured over a Braggs scattering angle range of 10° to 80°. Table 1 shows the lattice parameters of refined values of synthesized $Ca_2MgSi_2O_7{:}Eu^{2+}$, Dy^{3+} powder sample. From the XRD peaks it is observed that the compound mostly in single phase, which is consistent with standard JCPDS pdf file number #77-1149 [8].

3.2 Estimation of Crystallite Size (D)

The dopant and codopant ions did not affect the host structure. The narrow peaks indicate the particle size is in nano meters. In comparison to the reference data, there seems to be a little shift in the XRD data towards the larger angle. The crystallite size (D) was derived from the XRD pattern through using Debye-Scherrer's numerical formula [9, 10].

$$D = k\lambda/\beta Cos\theta \quad (3)$$

Where k (0.94) is the Debye-Scherrer constant, D is the crystallite size for the (hkl) plane, λ is the wavelength of the incident X-ray radiation [Cu-K_α (λ= 0.154056 nm)], β is the full width at half maximum (FWHM) in radiations, and θ is the corresponding angle of Bragg diffraction. The crystallite size (D) have calculated as ~42 nm using Debye-Scherrer's numerical formula. The lattice parameters of synthesized $Ca_2MgSi_2O_7$: Eu^{2+}, Dy^{3+} Sample have shown in Table: 1.

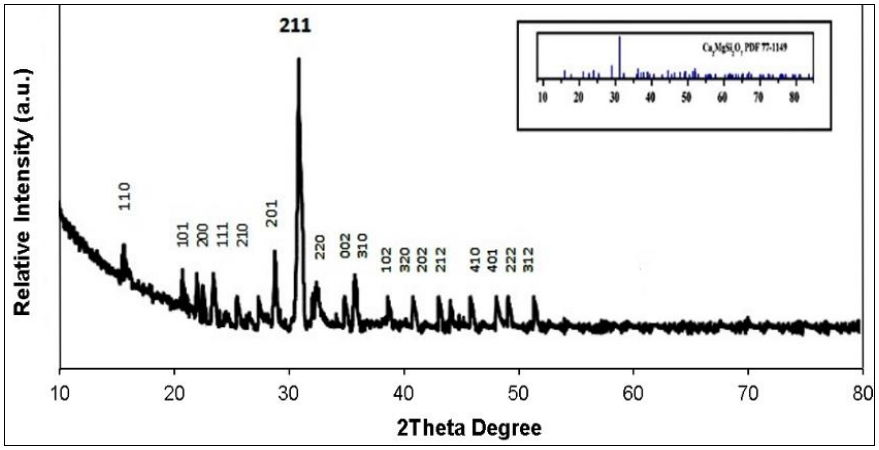

Fig 1: Powder X-ray Diffractogram Images of Synthesized Phosphor

Table 1: Lattice Parameters of Synthesized $Ca_2MgSi_2O_7$: Eu^{2+}, Dy^{3+} Sample [11]

Lattice Parameters	Values
Crystal Structure	Tetragonal
Phase Structure	Akermanite [$M_2T^1T^2_2O_7$]
Crystallography Group Member	Melilite
Space Group	$P\bar{4}21m$
Lattice Constants	a = 7.8071Å, b = 7.8071Å, c =4.9821Å a = β = γ = 90^0
Average Crystallite Size D (in nm)	~42nm
Prominent Peak (2θ)	31.24
Cell Volume (V)	303.663 $(Å)^3$
Colour	White

Due to distortion in the $Ca_2MgSi_2O_7$ host crystal lattice, dopant Eu^{2+} substitutes Ca^{2+} ions when it enters the host lattice and occupies Ca^{2+} lattice sites. Eu^{2+} has taken over former location of Ca^{2+} ions, while original location of Ca^{2+} ions has been changed. It's hard for Eu^{2+} ions to incorporate the tetrahedral [MgO_4] or [SiO_4] symmetry but it can easily incorporate octahedral [CaO_8] sites [12]. A typical feature of the IR spectrum is the observed influence of the vibration from the doping material Eu^{2+} in the $Ca_2MgSi_2O_7$:Eu^{2+}, Dy^{3+} host structure. Sharma *et al*. have reported that the dysprosium [Dy^{3+}] ions do not completely occupy two other tetrahedral sites, namely magnesium [Mg^{2+}] & silicon [Si^{4+}] ions. Therefore, [Ca^{2+}] lattice sites can occupy two alternative lattice sites, the six coordinated [Ca^{2+}] site [CaO_6 (Ca (I) site)] and the eight coordinated [Ca_{2+}] site [CaO_8 (Ca (II) site)]. We have also observed that the Mg^{2+} [MgO_4], and Si4+ [SiO_4] also evident, other two independent positive ions (i.e. cation) in the crystal lattice site. Both, [Mg^{2+}] and [Si^{4+}] cations clearly occupy in the tetrahedral lattice sites [13]. The Specific role of Dy^{3+} ions is to enhance ling persistent luminescence.

3.3 Analysis of Fourier Transform Infrared Spectroscopy (FTIR)

The identification of both organic and inorganic chemicals has been successfully accomplished using Fourier transform infrared spectroscopy (FTIR) [14]. FTIR is frequently used to examine organic compounds, which primarily underwent two sorts of modifications: Bond length changes brought on by stretching vibrations and bond angle changes brought on by bending vibrations. An inorganic compound's physical characteristics are represented by its infrared spectrum. Now that it has become well known, FTIR spectroscopy has advanced significantly in its ability to characterise materials. The IR spectra of Eu^{2+}-doped and Dy^{3+}-codoped $Ca_2MgSi_2O_7$ phosphor in the range of 4000 to 400 cm^{-1} are shown in Fig.2. Spectroscopically, the middle infrared region (4000–400 cm^{-1}) is extremely useful for the study of organic and inorganic compounds. The Infra-red zone of the electromagnetic spectrum extends from 100 µm to 1µm wavelength.

The wave-number of 3457.56 cm^{-1} is due to the O-H stretching mode in sintered phosphor is might be due to presence of moisture through environment. The band at 1774.57cm^{-1} can be ascribed to the existence of little quantity of the calcite [14]. The stretching around 1774.57 cm^{-1} is assigned to CO_3^{2-} modes. The free CO_3^{2-} modes (asymmetric stretching) has a D3h symmetry (trigonal planar) and its spectrum is dominated around the band at 1800 to 1700 cm^{-1} in $Ca_2MgSi_2O_7$:Eu^{2+}, Dy^{3+} phosphor is due to the presence of carbonate (raw material) [14, 15]. The FTIR spectrum of $Ca_2MgSi_2O_7$: Eu^{2+}, Dy^{3+} shows a vibration band at 1642.62 and 1484.35 cm^{-1}, which indicate the influence of Eu^{2+} ions. The vibration band of 1642.62 cm^{-1} are assigned due to the Mg^{2+} ions, because of the same of distortion in the $Ca_2MgSi_2O_7$ host crystal lattice. The bending of the sharp peaks in the region of 1484.35 cm^{-1} are assigned due to the bending of Ca^{2+}. Peak at 683.76 cm^{-1} may also be assigned to Ca-O bending vibrations and there was shift of bands at 739.32cm^{-1} are allocated to the vibration in the calcium [Ca^{2+}] ions [16]. Gou *et al*. [16] mentioned that the absorption bands, positioned at the wave-number 1326.71, 1065.43, 987.51, 946.62, 857.19 cm^{-1} is due to the vibration modes for the deformation of (Si-O_b-Si) and (Si-O_{nb}) stretching modes.

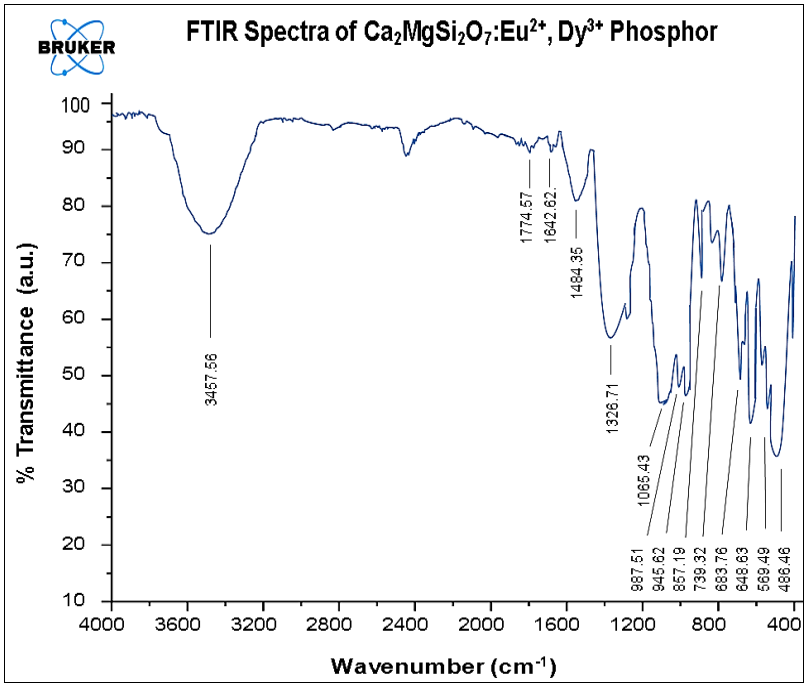

Fig 2: FTIR Spectra of Synthesized $Ca_2MgSi_2O_7:Eu^{2+}, y^{3+}$ Phosphor

The wave-number 739.32, 683.76, 648.63, 569.49 cm^{-1} are arising due to the (Si-O-Si) bending modes and the wave-number 481.56 cm^{-1} are based on the (Si-O-Si) bending modes and tetrahedral Si^{4+} lattice sites lie at 683.76, 857.19, 987.51 and 1065.43 cm^{-1}. The wave-number 486.46cm^{-1} are based on the Mg-O modes. In synthesized $Ca_2MgSi_2O_7:Eu^{2+}$, Dy^{3+} phosphor; Mg^{2+} and Si^{4+} ions occupy the tetrahedral sites [17-19].

Table 1: Functional Group, Finger Print and Infra-Red Frequencies Observed in Wave-number (cm^{-1}) with their Related Bonds

No.	Functional Group	Related Group Name	Frequency (in cm^{-1})
1.	O– H	Hydroxyl	3457.56
2.	CO_3^{2-}	Carbonate	1774.57
3.	Mg^{2+}	Magnesium	1642.62
4.	Ca^{2+}	Calcium	857.19, 739.32, 1484.35
5.	$Si - O_b - Si$	Silicate	1326.71
6.	$Si - O_b - Si$	Silicate	1065.43
7.	$Si - O_{nb}$	Silicate	987.51, 945.62
8.	$Si - O_b - Si$	Silicate	683.76, 648.63
9.	$Si - O_b - Si$	Silicate	569.46
10.	$Mg - O$	Magnesium Oxide	486.46
11.	Ca-O	Calcium Oxide	683.76
12.	Eu^{2+}	Europium	1642.62,1484.35
13.	Si^{4+}	Silicate	683.76, 857.19, 987.51

Applications of FTIR

The application of this FTIR technique is widely used, and it is notably preferred in the manufacturing of polymers, fibres, pharmaceuticals, medical devices, food, and chemicals. The IR spectrum is linked to molecule vibrations that are unique to each drug, just like a fingerprint is necessary for a specific person. With slight to no specimen preparation, it is possible to measure IR microscopes with amplitudes up to 10µm**.**

3.4 Analysis of Photoluminescence (PL) Spectrum

The photoluminescence (PL) spectra including with excitation and emission spectra of prepared $Ca_2MgSi_2O_7:Eu^{2+}$, Dy^{3+} phosphors with fixed dopant concentration of (0.5 mol %) Europium [Eu^{2+}] ions and codopant concentration of (2 mol %) of Dysprosium [Dy^{3+}] ions have been shown in Fig. 3(a) and 3(b). Eu^{2+}-doped and Dy^{3+}-codoped phosphors showed strong absorption in the UV band and emitted a bright green light when excited by UV light. At room temperature, the excitation and emission spectra of synthesized phosphor have been recorded. It was evidently examined at that the emission intensity increases with an increase in Dy^{3+} concentration, reaches an ideal value (2 mol %), and then decreases with an increase in Dy^{3+} concentration afterward, indicating that concentration quenching has occurred. The shapes and bands of the emission spectra are the same, but the intensities differ.

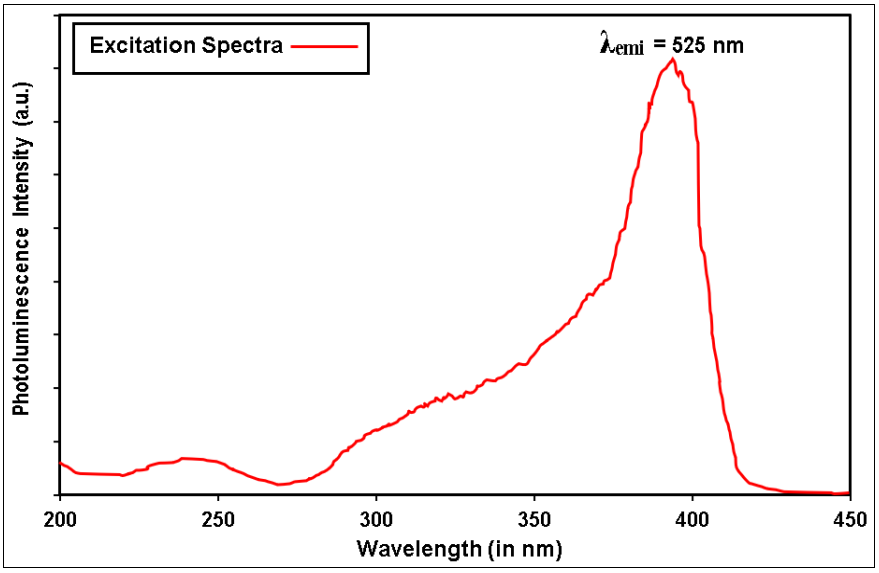

Fig 3 a): PLE Spectrum of Synthesized $Ca_2MgSi_2O_7:Eu^{2+}$, Dy^{3+} Phosphor monitored under 525nm wavelength

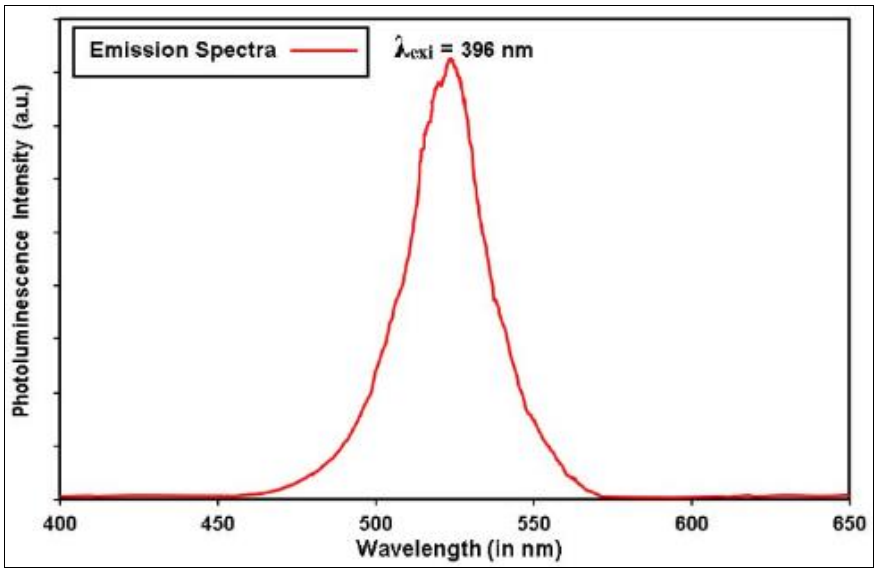

Fig 3 b): PL Emission Spectrum of Synthesized $Ca_2MgSi_2O_7:Eu^{2+}$, Dy^{3+} Phosphor under 396nm Excitation

Whenever the results revealed that the 200 to 450 nm region of the broadband excitation spectrum was observed and emission spectra were recorded in the range of 400 to 650 nm. The excitation broad band due to transitions of $^8S_{7/2}$ ($4f^7$) ground state to the excited state $4f^65d^1$ [$^8S_{7/2}$ ($4f^7$) → $4f^65d^1$] configuration was observed under the ultra violet excitation [20-23]. The excitation spectrum of the bright green fluorescence (λ_{em} = 525 nm) shows signal broad band with their peak situated at about 396 nm, respectively, which are due to the crystal field splitting of the Eu^{2+} d orbital. Under the excitation of 396 nm, the emission spectrum shows a strong band with a peak at about 525 nm, which corresponds to 4f–5d transition of Eu^{2+} ions. It is proposed that the compositional variation seems to have little impact on the crystal field because the crystal field can have a considerable impact on the $4f^65d^1$ electron states of Eu^{2+} ions. The intensity of the absorption at 396 nm, which is well suited with near-UV LED chip, is also favorable for pc-LEDs to produce white light emission.

According to our investigation, the bright green light emission at 525nm, which corresponds to ($^4F_{9/2}$→$^6H_{13/2}$) transitions and this luminescence emission belongs to hypersensitive transition with J=2, which is strongly based on surrounding of dysprosium [Dy^{3+}] ions. In our photoluminescence [PL] measurement, there is no other luminescence emission occurred in the presence of both Dy^{3+} ions and Eu^{3+} ions, which suggests that the Europium ions have undergone a reduction process (i.e. Eu^{3+} to Eu^{2+} ions) completely. In co-doped systems with Eu^{2+} and Dy^{3+}, the Eu^{2+} is generally perceived of as an activator and the Dy^{3+} as creating some traps for electrons or holes [24, 25], and enhance the long persistent luminescence.

3.5 Analysis of CIE Chromaticity Coordinates

The most important aspect through using materials or phosphors is their luminescent colour. The CIE chromaticity coordinates diagram is employed in order to assess and accurately describe the colour emission of any phosphors or materials [26]. Observing the emission spectra of the phosphors allowed researchers to identify

this coordinate. The spectral energy distribution is used to calculate the Commission Internationale de l'Eclairage (CIE) coordinates (1931 chart) using GO-CIE software, which are depicted in Fig. 4. The calculated spectral Locus CIE coordinates of the $Ca_2MgSi_2O_7:Eu^{2+}$, Dy^{3+} phosphor is X = 0.1141, and Y = 0.8262. From the CIE chromaticity co-ordinates, the luminescent emission colour is in bright green region indicating that this can be useful as green component phosphors under near UV excitation for the generation of white light.

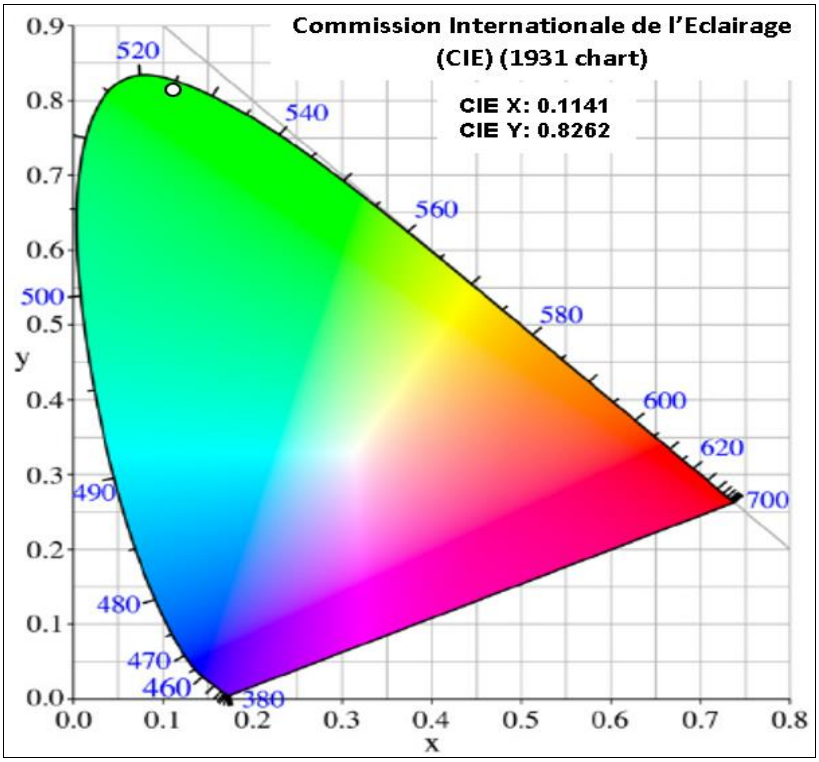

Fig 4: CIE co-ordinates of $Ca_2MgSi_2O_7:Eu^{2+}$, Dy^{3+} phosphor depict on 1931 chart

4. Conclusions

In summary, $Ca_2MgSi_2O_7:Eu^{2+}$, Dy^{3+} phosphor was synthesized successfully via a high-temperature traditional solid-state reaction technique. From XRD studies the compound is mostly in single phase. The crystallite size (D) have calculated as ~42 nm using Debye-Scherrer's numerical formula. In-depth explanations of various functional group ranges in organic compounds and nanomaterials are presented. The FTIR results confirms that the synthesized phosphor has a better phase formation and this phosphor contains chemical bonds and Functional group such as (O-H), (Mg-O), (Si-O), (Ca-O), (O-Si-O) and (CO_3^{2-}), as well as (SiO_4). Consequently, the implementation of FTIR in several branches of science has been investigated. Exponentially advancing is FTIR's capability to analyze chemical and biological substances. The material on the substrate's surfaces may additionally be analysed using this technique. The aluminates' luminescence characteristics degrade as soon as they are exposed to water, which restricts their application as a pigment in luminous paints. The completely dominant colour for luminescence in photoluminescence spectra is bright green. The prepared phosphor was excited at 396 nm and their corresponding emission spectra were recorded at bright green (525 nm) spectral line peaking due to the $^4F_{9/2} \rightarrow {}^6H_{13/2}$ transitions, which suits the visual perception of the human eye very well. The CIE chromaticity coordinate of the $Ca_2MgSi_2O_7:Eu^{2+}$, Dy^{3+} phosphor was found to be (X= 0.1141, Y = 0.8262) in higher green color purity region. The results in this work demonstrate that this phosphor is expected to be promising candidates for application in solid state lighting display devices and near-UV LEDs.

5. Applications

The favourable features for applications likewise near UV-LED conversion phosphor, drug delivery, cancer therapy, tissue engineering, bone material, detection of cancer diseases, solid-state lighting devices, display devices, white light emitting diodes and Image processing of computer science.

6. Acknowledgement

We are heartily grateful to Dept. of physics, Dr. Radha Bai, Govt. Navin Girls College Mathpara Raipur (C.G.), providing the facility of muffle furnace and other essential research equipments. We gratefully acknowledge the kind support for the facility of XRD analysis Dept. of Metallurgical Engineering and FTIR analysis Dept. of physics, NIT Raipur (C.G.). Authors are also thankful to Dept. of physics, Pt. Ravishankar Shukla University, Raipur (C.G.) for providing us the facility of photoluminescence spectral analysis including with excitation and emission spectra. We are special thankful to Mr. Sanjay Deshmukh and Mr. Suresh Dua for characterization study and data measurements in NIT Raipur.

7. Competing Interests
Authors have declared that no competing interests exist in present investigation.

8. Funding Source
All the characterization and measurement are carried out by self-funding source.

9. References
1. Fan M, Dai D, Huang B. Fourier transform infrared spectroscopy for natural fibres. Fourier transform-materials analysis,2012:3:45-68.
2. Sharma A, Singh JP, Won SO, Chae KH, Sharma SK, Kumar S. Introduction to X-ray absorption spectroscopy and its applications in material science. Handbook of Materials Characterization. Springer International Publishing AG, part of Springer Nature, 2018, 497-548.
3. Kirk RE, Othmer DF. Encyclopedia of Chemical Technology. The Inter science Encyclopedia. Inc., New York,1953:2:480-485.
4. Zhang Z, Wang Y. UV-VUV excitation luminescence properties of Eu^{2+}-doped $Ba_2MSi_2O_7$ (M= Mg, Zn). Journal of the Electrochemical Society, 2006, 154-J62.
5. Jiang L, Chang C, Mao D, Feng C. Concentration quenching of Eu^{2+} in $Ca_2MgSi_2O_7$: Eu^{2+} phosphor. Materials Science and Engineering: B,2003:103:271-275.
6. Shannon RD. Revised effective ionic radii and systematic studies of interatomic distances in halides and chalcogenides. Acta crystallographica section A: crystal physics, diffraction, theoretical and general crystallography,1976:32:751-767.
7. Furusho H, Hölsä J, Laamanen T, Lastusaari M, Niittykoski J, Okajima Y, *et al*. Probing lattice defects in $Sr_2MgSi_2O_7$: Eu^{2+}, Dy^{3+}. Journal of luminescence,2008:28:881-884.
8. JCPDS PDF File No. 17-1149, JCPDS International Center for Diffraction Data.
9. Birks LS, Friedman H. Particle size determination from X-ray line broadening. Journal of Applied Physics,1946:17:687-692.
10. Scherrer P. Bestimmung der Grösse und der inneren Struktur von Kolloidteilchen mittels Röntgenstrahlen. Nachrichten von der Gesellschaft der Wissenschaften zu Göttingen, mathematisch-physikalische Klasse, 1918, 98-100.
11. Sharma S, Dubey SK, Diwakar AK, Pandey S. Novel white light emitting ($Ca_2MgSi_2O_7$: Dy^{3+}) Phosphor. Journal of Materials Science Research and Reviews,2021:8:164-171.
12. Jiang L, Chang C, Mao D, Feng C. Luminescent properties of $Ca_2MgSi_2O_7$ phosphor activated by Eu^{2+}, Dy^{3+} and Nd^{3+}. Optical Materials,2004:27:51-55.
13. Sharma S, Dubey SK. Significant Contribution of Deeper Traps for Long Afterglow Process in Synthesized Thermoluminescence Material. J Miner Sci Materials,2022:3:1-6.
14. Sharma S, Dubey SK, Diwakar AK. Luminescence investigation on $Ca_2MgSi_2O_7$:Eu^{2+}, Dy^{3+} phosphor. International Journal of Materials Science,2021:2:08-15.
15. Martinez A, Izquierdo-Barba I, Vallet-Regi M. Bioactivity of a $CaO{-}SiO_2$ binary glasses system. Chemistry of Materials,2000:12:3080-3088.
16. Gou Z, Chang J, Zhai W. Preparation and characterization of novel bioactive dicalcium silicate ceramics. Journal of the European Ceramic Society,2005:25:1507-1514.
17. Frost RL, Bouzaid JM, Reddy BJ. Vibrational spectroscopy of the sorosilicate mineral hemimorphite $Zn_4(OH)_2Si_2O_7{\cdot}H_2O$. Polyhedron,2007:26:2405-2412.
18. Chandrappa GT, Ghosh S, Patil KC. Synthesis and Properties of Willemite, Zn_2SiO_4, and M^{2+}: Zn_2SiO_4 (M= Co and Ni). Journal of Materials Synthesis and Processing,1999:7:273-279.
19. Makreski P, Jovanovski G, Kaitner B, Gajović A, Biljan T. Minerals from Macedonia: XVIII. Vibrational spectra of some sorosilicates. Vibrational Spectroscopy,2007:44:162-170.
20. Salim MA, Hussin R, Abdullah MS, Abdullah S, Alias NS, Fuzi SA, *et al*. The local structure of phosphor material, $Sr_2MgSi_2O_7$ and $Sr_2MgSi_2O_7$: Eu^{2+} by infrared spectroscopy. Solid State Science and Technology,2009:17:59-64.
21. Wu H, Hu Y, Zeng B, Mou Z, Deng L. Tunable luminescent properties by adjusting the Sr/Ba ratio in $Sr_{1.97-x}Ba_xMgSi_2O_7$:Eu^{2+} 0.01, Dy^{3+} 0.02 phosphors. Journal of Physics and Chemistry of Solids,2011:72:1284-1289.
22. Shi C, Fu Y, Liu B, Zhang G, Chen Y, Qi Z, *et al*. The roles of Eu^{2+} and Dy^{3+} in the blue long-lasting phosphor $Sr_2MgSi_2O_7$: Eu^{2+}, Dy^{3+}. Journal of luminescence,2007:122:11-13.
23. Lin L, Zhonghua ZH, Zhang W, Zheng Z, Min YI. Photo-luminescence properties and thermo-luminescence curve analysis of a new white long-lasting phosphor: $Ca_2MgSi_2O_7$:Dy^{3+}. Journal of Rare Earths,2009:27:749-752.
24. Lin Y, Zhang Z, Tang Z, Wang X, Zhang J, Zheng Z. Luminescent properties of a new long afterglow Eu^{2+} and Dy^{3+} activated $Ca_3MgSi_2O_8$ phosphor. Journal of the European Ceramic Society,2001:21:683-685.
25. Liu B, Shi C, Yin M, Dong L, Xiao Z. The trap states in the $Sr_2MgSi_2O_7$ and (Sr, Ca) $MgSi_2O_7$ long afterglow phosphor activated by Eu^{2+} and Dy^{3+}. Journal of alloys and compounds,2005:387:65-69.
26. CIE. International Commission on Illumination. Publication CIE no. 15 (E-1.3.1),1931.